International Journal of Modern Physics D

AGN torus threaded by large scale magnetic field

A. Dorodnitsyn *

Laboratory for High Energy Astrophysics, NASA Goddard Space Flight Center, Code 662, Greenbelt, MD, 20771, USA;

T. Kallman

Laboratory for High Energy Astrophysics, NASA Goddard Space Flight Center, Code 662, Greenbelt, MD, 20771, USA;

Received Day Month Year
Revised Day Month Year

Large scale magnetic field can be easily dragged from galactic scales towards AGN along with accreting gas. There, it can contribute to both the formation of AGN "torus" and help to remove angular momentum from the gas which fuels AGN accretion disk. However the dynamics of such gas is also strongly influenced by the radiative feedback from the inner accretion disk. Here we present results from the three-dimensional simulations of pc-scale accretion which is exposed to intense X-ray heating.

Keywords: accretion, accretion disks - Galaxies: active - Galaxies: Seyfert - magnetic fields: - magnetohydrodynamics (MHD)

1. Introduction

The location of the torus near 1 pc from the black hole is is supported by IR imaging and by the fact that 1 pc is close to the dust sublimation radius. If so, an explanation is needed for the apparent geometrical thickness of the torus. suggestion that Seyfert 2 galaxies suffer from enhanced extinction compared to Seyfert 1 galaxies was made by Rowan-Robinson (1977) based on the infrared observations. However, it was not until the seminal work of Antonucci (1984) and Antonucci & Miller (1985) that key evidence was collected from studies based on optical spectropolarimetry. The detection of broad permitted lines in the polarized UV and optical spectra of the nearby, luminous Seyfert 2 galaxy NGC 1068 confirmed that a bright, Seyfert 1 core is hidden behind optically thi ck, obscuring material. Diverse torus models have been proposed to interpret AGN observations in the infrared.

Since the temperature of an accretion disk at pc-scale is approximately 100-1000 K, a disk will be very thin. A warped disk model has been put forward to explain

*University of Maryland, Baltimore County (UMBC/CRESST), Baltimore, MD 21250, USA; Space Research Institute, 84/32, Profsoyuznaya st., Moscow, Russia; dorodnitsyn@gmail.com

the apparent thickness in a global sense, in which various mechanisms, including irradiation can potentially produce global warps in a locally thin disk (Phinney, 1989; Sanders et al., 1989).

Models in which the torus is intrinsically geometrically thick involve rotating stationary tori or assume some kind of an outflowing accretion disk wind. Geometrically thick flows can be associated with a global magnetic field which allows an magneto-hydrodynamic (MHD) wind (Elitzur & Shlosman, 2006; Konigl & Kartje, 1994) or directly supports a quasi-static torus (Dorodnitsyn & Kallman, 2017; Lovelace et al., 1998), or a combination of radiative and magnetic driving (Emmering et al., 1992; Everett, 2005; Keating et al., 2012; Konigl & Kartje, 1994). Such hydromagnetic models require large (poloidal) magnetic flux to support a wind, along with a thin equatorial disk as a boundary condition. Self-similar hydro-magnetically driven winds studied by Everett (2005); Keating et al. (2012) predict the IR spectral energy distributions (SED) that are approximately the right shape compared to the composite of the optically luminous quasars. These models are based on an assumed The unification paradigm of Active Galactic Nuclei (AGN) implies the existence of a geometrically thick belt of matter which wraps and hides the inner, most luminous region of AGN from viewing close to the equatorial plane (Antonucci, 1984; Antonucci & Miller, 1985; Rowan-Robinson, 1977). This can explain the dichotomy of Type I and Type II AGNs and Quasars, attributing their differing appearance to the geometrical positioning of an AGN with respect to an observer.

Observations favor this model, but the mechanism that actually supports such a geometrically thick structure is not determined. In the absence of efficient cooling, the virial theorem predicts that gas which is orbiting the black hole at the radius of the putative torus, $r \simeq 1\,\mathrm{pc}$ will have temperature $T_{\mathrm{vir,g}} \simeq 10^6$ K for a $10^7 M_\odot$ black hole. Dust at such temperatures is destroyed by sputtering, while the presence of dust in the torus is supported by abundant observational evidence. Emission from warm dust manifests itself in a broad hump in the spectral energy distribution (SED) in the $\sim 1-10\mu$ wavelength band Interferometric observations provide direct evidence of warm, multi-temperature dust at parsec scales in a growing sample of nearby type II and type I AGNs, including NGC 1068, the Circinus galaxy and others (i.e. Hönig et al., 2012; Poncelet et al., 2006; Raban et al., 2009; Tristram et al., 2014) Observations of ionization and scattering cones also indicate the existence of a toroidal obscuring structure (eg. Pogge & De Robertis, 1993; Wilson, 1996; Zakamska et al., 2005).

A different view on torus where it is dynamics - "windy torus", was proposed by (Chan & Krolik, 2016; Dorodnitsyn et al., 2011; Dorodnitsyn & Kallman, 2012; Dorodnitsyn et al., 2012). Simulations show that IR pressure support works most efficiently in AGNs with inferred bolometric luminosity $L \gtrsim 0.1\,L_{\mathrm{edd}}$, where L_{edd} is the Eddington luminosity.

The torus is also the most likely source of gas for the inner accretion disk and the fueling of the black hole. This raises the important question of the nature of the mechanism that provides angular momentum redistribution. This includes the

mechanism which operates on scales larger than the torus, and brings gas into the torus, and also the mechanisms operating within the torus.

On galactic scales, gas can be funneled towards the center as a result of a galaxy merger, leading to the development of the bar instability (Shlosman et al., 1990, 1989). Observations indicate the existence of large scale magnetic fields on galactic scales (i.e. Beck, 2011; Beck & Wielebinski, 2013), and the inflow can transport magnetic flux from the inner parts of the host galaxy towards the torus. The importance of magnetic flux can be inferred from the following approximate arguments: assume the spherically-symmetric shell of gas located within the BH sphere-of-influence, falls radially at roughly a free-fall velocity and with a constant accretion rate. Then assuming perfect conductivity, conservation of magnetic flux implies $B_r \sim r^{-2}$, where B_r is the radial component of the magnetic field. The gas internal energy scales as $\rho v^2/2 \sim r^{-5/2}$. The density profile is then $\rho \sim r^{-3/2}$ and the distance from the BH where magnetic field becomes dynamically important can be estimated from energy equipartition arguments (Bisnovatyi-Kogan & Lovelace, 2000; Bisnovatyi-Kogan & Ruzmaikin, 1974): $r_m = r_{\rm out}^{8/3} B_{\rm out}^{4/3} \dot{M}_\odot^{-2/3} (GM_{\rm BH})^{-1/3} \simeq 81 B_{10}^{4/3} R_{100}^{8/3} \dot{m}_{0.01}^{-2/3} M_7^{-1/3}$pc, where B_{10} is the galactic magnetic field scaled to $10\,\mu$G, R_{100} is the outer AGN radius $r_{\rm out}$ in units of 100 pc, the accretion rate, $\dot{m}_{0.01}$ is scaled to $10^{-2} M_\odot$/yr, and M_7 is the mass of the BH in $10^7 M_\odot$. Parsec-scale magnetic field loops that were small-scale in the galactic disk will dominate the geometry in the torus region. This illustrates the potential dynamical importance of magnetic field in the torus. If so, in such a magnetized rotating torus, orbital shear can lead to magnetic instability in which angular momentum is redistributed via magnetic stresses. In the inner accretion disk MHD turbulence driven by the MRI instability (Balbus & Hawley, 1991) is currently the most likely mechanism for angular momentum transport leading to accretion Significant insight here comes from local, shearing box simulations. An important result of such simulations is that the presence of net magnetic flux in the simulation box essentially guarantees the efficacy of the MRI. Surprisingly little effort has been devoted to the investigation of the role of large scale magnetic fields in the context of the AGN outer disk/torus. Lovelace et al. (1998) derived a model of a magnetically-supported, thick torus assuming that the magnetic field is produced by an equatorial current loop and making a number of other simplifications suitable for an approximate analytic model. A different class of magnetic models associate the torus with a geometrically thick flow, driven either by magnetic driving (Elitzur & Shlosman, 2006; Fukumura et al., 2010; Konigl & Kartje, 1994) alone, or in combination with radiation pressure (Emmering et al., 1992; Everett, 2005; Keating et al., 2012). To launch the wind these models rely on an ordered global magnetic field with foot-points originating on a thin disk.

The plan of the paper is as follows: In the first part we study an analytic model of a magnetically supported torus. Our approximate solution is based on the exact solution of the Grad-Shafranov equation - the solution initially derived by Soloviev for the toroidal equilibrium in Tokamaks.

In this paper we report the results of three- dimensional numerical simulations of the X-ray illuminated torus threaded by global magnetic field. We show that the evolution of a physically realistic torus is sensitive to these assumptions about the global field distribution, and that this affects the obscuring properties as well. In the results section we summarize many of the characteristics of the torus such as its dynamics, obscuring properties, accretion-rate etc. We conclude with discussion of the implications of our models for understanding the torus dynamics, and potential limitations associated with the our assumptions.

2. MHD Equations for AGN Torus

We model the torus using three-dimensional, ideal MHD equations describing magnetized gas susceptible to radiative heating and cooling in a Newtonian gravitational potential:

$$\partial_t \rho + \nabla \cdot (\rho\, \mathbf{v}) = 0, \tag{1}$$

$$\partial_t(\rho \mathbf{v}) + \nabla \cdot (\rho \mathbf{v}\mathbf{v} - \mathbf{B}\mathbf{B} + P^* \mathbf{I}) = -\rho \frac{G\, M_{\rm BH}}{r^2}\, \hat{\mathbf{r}}, \tag{2}$$

$$\partial_t E + \nabla \cdot [(E + P^*)\mathbf{v} - \mathbf{B}(\mathbf{B}\cdot\mathbf{v})] = -\rho \mathbf{v} \cdot \frac{G\, M_{\rm BH}}{r^2}\ \hat{\mathbf{r}} - \rho\, \mathcal{L}, \tag{3}$$

$$\partial_t \mathbf{B} + \nabla \cdot (\mathbf{v}\cdot\mathbf{B} - \mathbf{B}\cdot\mathbf{v}) = 0, \tag{4}$$

where density, $\rho = n\, m_{\rm u} \mu$ ($m_{\rm u} = 1\,{\rm amu} \simeq m_p$ is the atomic mass unit; m_p is the proton's mass); we also adopt $\mu = 1$ for the mean mean molecular weight. $P^* \equiv P + (\mathbf{B}\cdot\mathbf{B})/2$ is the total pressure, E is the total energy density, $E \equiv e + \rho(\mathbf{v}\cdot\mathbf{v})/2 + (\mathbf{B}\cdot\mathbf{B})/2$, where e is the internal energy density. A polytropic equation of state is assumed: $P = (\gamma - 1)\, e$, where P is the gas pressure, γ is the ratio of specific heats. Additional notation includes r, and $\hat{\mathbf{r}}$ - the usual spherical radius and the spherical radial unit vector. Interaction with radiation is included in the form of the X-ray cooling-heating function, $\mathcal{L}\left[{\rm erg\,g^{-1}\,s^{-1}}\right]$ in The detailed meaning of each quantity is given in (Dorodnitsyn & Kallman, 2017)

3. Results

Our models can be broadly divided with respect to the relative strength of the large-scale B-field. In the SOL model (see Dorodnitsyn, Kallman 2107) magnetic field confines the initial torus while in the TOR simulation it is fully contained within the torus body. The large scale magnetic field in the SOL simulation is effective in smoothing the contrast in specific angular momentum l, so that this quantity remains close to its local Keplerian value, $l_{\rm k}$. This is not true for the TOR simulations. Figure 1 shows the distribution of $\log(\rho)$. In the TOR solutions, l spans the full range, from $l \sim l_{\rm k}$ near the inner domain boundary to an approximately half of $l_{\rm k}$ at larger R. The rotation velocity, v_ϕ remains nearly Keplerian inside a

significant part of the torus. This is more true close to the equator. In the torus throat most of the low density gas is sub-Keplerian.

Different topologies of the initial field results in different levels of MRI- driven stirring of the torus interior. The density near the disk funnel is naturally higher than the density in a smooth disk of the same mass. Shielding depends on the optical depth of the obscuring region, $\sim \bar{\rho}\,\delta l$. In the SOL solution there is little gas in the central hole, and thus the characteristic length scale, δl is smaller, but this is more than compensated by the increase of the density in this region, $\bar{\rho}$ due to compression of the funnel walls. Correspondingly, the SOL solution shows more efficient shielding from X-rays. Thus, the gas in TOR solution is considerably hotter, $T \simeq 10^5$K than in SOL case, $T \simeq 10^4$K. Near the axis the gas is very hot, almost virialized: in SOL case it is $T \simeq 10 \times 10^7$K and in TOR case it is $T \simeq 2.5 \times 10^6$K. Angular dependence of the optical depth manifests itself in "ionization cones".

Mass-loss rate is noticeably influenced by the distribution of the B-flux in the torus funnel. The torus sheds more mass via $\dot{M}_{\rm w}$ than from $\dot{M}_{\rm a}$. Excretion is expected as angular momentum is transferred outwards by both the wind and equatorial outflow. After $T \sim 2 \times 10^4$ yrs in both runs the mass-loss rate enters a regime in which $\dot{M}_{\rm a}$ is fluctuating within a range; in case of SOL: $\dot{M}_{\rm a} \simeq 10^{-4} - 10^{-3}\, M_\odot\,{\rm yr}^{-1}$, and TOR: $\dot{M}_{\rm a} \simeq 10^{-1} - 3 \times 10^1\, M_\odot\,{\rm yr}^{-1}$. There is no obvious increasing or decreasing trend in average mass-accretion rate, $\langle \dot{M}_{\rm a} \rangle$. The largest variability scale of the TOR is about 10^4 yrs while in the SOL it is much smaller, about 10^3 yrs. The variability amplitude in the SOL solutions is generally smaller than in the TOR solutions. In both cases the wind mass-loss rate, $\dot{M}_{\rm w} \simeq 0.01 - 0.1 M_\odot\,{\rm yr}^{-1}$. Notice that for our model parameters, the Eddington mass-accretion rate, $\dot{M}_{\rm a,Edd} \simeq 0.1 M_\odot\,{\rm yr}^{-1}$ where we assumed the efficiency of accretion, $\epsilon = 0.1$. The accretion rate in SOL and TOR runs almost always stays below this level with the excess energy removed by winds.

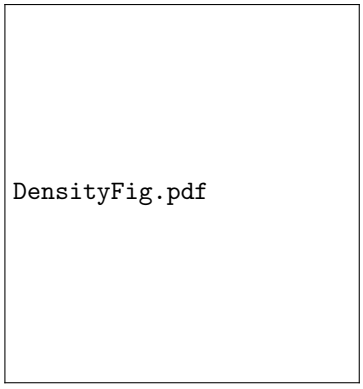

Fig. 1. Density distribution at $t = 10 t_{\rm orb}$

4. Conclusions

Our torus model features a poloidal magnetic field which is partly trapped inside the torus where it contributes to its vertical support against gravity. A second model also has a significant magnetic flux outside the torus. We argue that both of these initial states may result from accretion of magnetized gas from galactic scales in which case a dynamically significant magnetic flux can accumulate in the inner regions of AGN as a result of magnetic field dragging from the galaxy.

References

Antonucci, R. R. J. 1984, ApJ, 278, 499
Antonucci, R. R. J., & Miller, J. S. 1985, ApJ, 297, 621
Balbus, S. A., & Hawley, J. F. 1991, ApJ, 376, 214
Beck, R. 2011, in American Institute of Physics Conference Series, Vol. 1381, American Institute of Physics Conference Series, ed. F. A. Aharonian, W. Hofmann, & F. M. Rieger, 117–136
Beck, R., & Wielebinski, R. 2013, Magnetic Fields in Galaxies, 641
Bisnovatyi-Kogan, G. S., & Lovelace, R. V. E. 2000, ApJ, 529, 978
Bisnovatyi-Kogan, G. S., & Ruzmaikin, A. A. 1974, Ap&SS, 28, 45
Chan, C.-H., & Krolik, J. H. 2016, ApJ, 825, 67
Czerny, B., & Hryniewicz, K. 2011, A&A, 525, L8
Czerny, B., Rózańska, A., & Kuraszkiewicz, J. 2004, A&A, 428, 39
Dorodnitsyn, A., Bisnovatyi-Kogan, G. S., & Kallman, T. 2011, ApJ, 741, 29
Dorodnitsyn, A., & Kallman, T. 2012, ApJ, 761, 70
Dorodnitsyn, A., Kallman, T., & Bisnovatyi-Kogan, G. S. 2012, ApJ, 747, 8
—. 2017, ApJ, 842, 43
Elitzur, M., & Shlosman, I. 2006, ApJ., Letters, 648, L101
Emmering, R. T., Blandford, R. D., & Shlosman, I. 1992, ApJ, 385, 460
Everett, J. E. 2005, ApJ, 631, 689
Fukumura, K., Kazanas, D., Contopoulos, I., & Behar, E. 2010, ApJ., Letters, 723, L228
Hönig, S. F., Kishimoto, M., Antonucci, R., Marconi, A., Prieto, M. A., Tristram, K., & Weigelt, G. 2012, ApJ, 755, 149
Keating, S. K., Everett, J. E., Gallagher, S. C., & Deo, R. P. 2012, ApJ, 749, 32
Konigl, A., & Kartje, J. F. 1994, ApJ, 434, 446
Lovelace, R. V. E., Romanova, M. M., & Biermann, P. L. 1998, A&A, 338, 856
Phinney, E. S. 1989, in NATO ASIC Proc. 290: Theory of Accretion Disks, ed. F. Meyer, 457–+
Pogge, R. W., & De Robertis, M. M. 1993, ApJ, 404, 563
Poncelet, A., Perrin, G., & Sol, H. 2006, A&A, 450, 483
Raban, D., Jaffe, W., Röttgering, H., Meisenheimer, K., & Tristram, K. R. W. 2009, MNRAS, 394, 1325
Rowan-Robinson, M. 1977, ApJ, 213, 635

Sanders, D. B., Phinney, E. S., Neugebauer, G., Soifer, B. T., & Matthews, K. 1989, ApJ, 347, 29
Sano, T., Inutsuka, S.-i., Turner, N. J., & Stone, J. M. 2004, ApJ, 605, 321
Shlosman, I., Begelman, M. C., & Frank, J. 1990, Nature, 345, 679
Shlosman, I., Frank, J., & Begelman, M. C. 1989, Nature, 338, 45
Tristram, K. R. W., Burtscher, L., Jaffe, W., Meisenheimer, K., Hönig, S. F., Kishimoto, M., Schartmann, M., & Weigelt, G. 2014, A&A, 563, A82
Tristram, K. R. W., & Schartmann, M. 2011, A&A, 531, A99
Wilson, A. S. 1996, Vistas in Astronomy, 40, 63
Zakamska, N. L., et al. 2005, AJ, 129, 1212